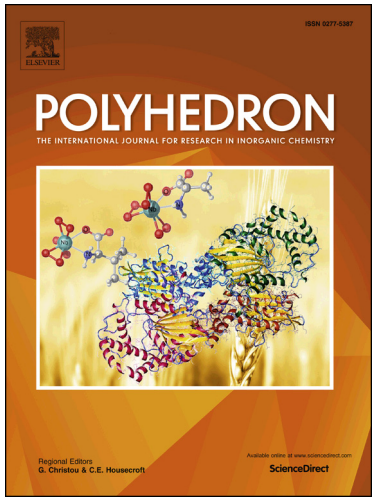


# Syntheses, structural diversity and thermal behavior of first row transition metal complexes containing potential multidentate ligands based on 2,6-diacetylpyridine and benzyl carbazate

Palanivelu Nithya, Jim Simpson, Subbiah Govindarajan

PII: S0277-5387(17)30709-X
DOI: https://doi.org/10.1016/j.poly.2017.11.009
Reference: POLY 12911

To appear in: *Polyhedron*

Received Date: 10 July 2017
Accepted Date: 6 November 2017

Please cite this article as: P. Nithya, J. Simpson, S. Govindarajan, Syntheses, structural diversity and thermal behavior of first row transition metal complexes containing potential multidentate ligands based on 2,6-diacetylpyridine and benzyl carbazate, *Polyhedron* (2017), doi: https://doi.org/10.1016/j.poly.2017.11.009

# Syntheses, structural diversity and thermal behavior of first row transition metal complexes containing potential multidentate ligands based on 2,6-diacetylpyridine and benzyl carbazate

Palanivelu Nithya[a], Jim Simpson[b] and Subbiah Govindarajan[a*]

[a]Department of Chemistry, Bharathiar University, Coimbatore 641 046, Tamil Nadu, India

[b]Department of Chemistry, University of Otago, Dunedin 9054, New Zealand

*Corresponding author: E-mail: drsgovind@yahoo.co.in

**Abstract**

The Schiff base ligand, N'-(1-{6-[1-(Benzyloxycarbonyl-hydrazono)-ethyl]-pyridin-2-yl}-ethylidene)-hydrazinecarboxylic acid benzyl ester (**$bc_2$-dap**), was synthesized by the reaction of 2,6-diacetylpyridine (dap) with benzyl carbazate (bc) in methanol. Also first row transition metal complexes of the general formula $[M(NCS)_2(bc_2\text{-dap})].nH_2O$; M = Mn (**1**), Fe (**2**), Co (**3**), Zn (**4**) or Co (**5**); n=0 (**1-4**) and n=1 (**5**), $[Fe(bc_2\text{-dap})(H_2O)_2].2Cl.4H_2O$ (**6**), $[Ni(NCS)_2(bc_2\text{-dap})].CH_3OH$ (**7**) and $[Co(NCS)_2(bc\text{-dap})]$ (**8**) have been synthesized using a template method and characterized by spectroscopic techniques and single crystal X-ray diffraction. Complexes **1**-**4** are isotypic, while compounds **1-6** comprises of discrete mononuclear units with pentagonalbipyramidal geometry. In contrast compounds **7** and **8** adopt octahedral and tetrahedral geometries, respectively. In all of the complexes **1-6**, the Schiff base acts as a pentadentate ligand that binds *via* the pyridine nitrogen, azomethine nitrogen and carbonyl oxygen atoms. The Schiff base ligand occupies the equatorial plane and isothiocyanate anions for **1-5** and water molecules for **6** occupy the axial positions. Compound **7** has octahedral geometry in which the Schiff base ligand acts as a tetradentate ligand and in this case one of the carbonyl oxygen atoms is not involved in coordination. Furthermore, the N-bound isothiocyanate anions

are coordinated as terminal ligands. In compound **8**, the Schiff base behaves as a bidentate ligand through the azomethine nitrogen and pyridine nitrogen atoms leading to a tetrahedral geometry with the remaining two sites are occupied by isothiocyanate ions. Thermal reactivity of the ligand and complexes (**1-8**) was studied by TG-DTA and the complexes all undergo endo- followed by exothermic decomposition to give metal oxides, whereas the ligand decomposes completely to give gaseous products.

*Keywords:* Benzyl carbazate, 2,6-diacetylpyridine, Schiff base complexes, Crystal structures, Thermal behavior

# Syntheses, structural diversity and thermal behavior of first row transition metal complexes containing potential multidentate ligands based on 2,6-diacetylpyridine and benzyl carbazate

Palanivelu Nithya[a], Jim Simpson[b] and Subbiah Govindarajan[a*]

[a] Department of Chemistry, Bharathiar University, Coimbatore 641 046, Tamil Nadu, India

[b] Department of Chemistry, University of Otago, Dunedin 9054, New Zealand

*Corresponding author: E-mail: drsgovind@yahoo.co.in

## 1. Introduction

Metal complexes containing esters of hydrazinecarboxylic acid, that is, carbazates have been of considerable interest due to their interesting thermal and structural properties [1-8]. Carbazates are interesting as ligands in view of their variety of potential oxygen and nitrogen donor atoms and these neutral molecules are expected to exhibit only one a common coordination mode, namely bidentate N, O-chelation. In recent years, we have explored the coordination chemistry of methyl and ethyl carbazates and have now turned our attention to benzyl carbazate ($NH_2NHCOOCH_2C_6H_5$, bc) that is structurally related to these alkyl carbazates. Further, the coordination chemistry of benzyl carbazate has not been explored extensively. Guerra *et al*. reported [9, 10] the syntheses, spectroscopic characterizations, DFT studies and cytotoxic activity of $[M(X)_2Cl_2]$ {where M = Pd or Pt, X = 4-methoxybenzylcarbazate (4-MC), benzyl carbazate (BC), 4-fluorophenoxyacetic acid hydrazide (4-FH), 3-methoxybenzoic acid hydrazide (3-MH) and *tert*-butyl carbazate (TC)}, $[M(EC)_2I_2]$ {M = Pd or Pt, EC = ethyl carbazate} and $[Pt(4\text{-}HH)_2I_2].2.5H_2O$ {4-HH = (4-hydroxy-phenyl)-acetic acid hydrazide (4-HH)}. Apart from its coordinating ability, benzyl carbazate can also undergo condensation reactions; the hydrazinic part of the terminal amine group reacts with the carbonyl groups of aldehydes or ketones to form Schiff bases. However,

Schiff bases and their metal complexes derived from benzyl carbazate have not been studied till date except our own recent reports [11-13] of Schiff bases derived from benzyl carbazate with alkyl and heteroaryl ketones and their metal complexes.

In the recent past, the coordination properties of 2,6-diacetylpyridine based Schiff base ligands have been investigated in detail and are shown to be particularly versatile in the variety of coordination modes that they adopt. Among such Schiff base ligand systems considerable interest has been shown in the coordination chemistry of metal complexes based on 2,6-diacetylpyridine with hydrazinic bases such as hydrazines [14-18], hydrazides [19-23], semicarbazides [24, 25] and thiosemicarbazides [26-32]. In addition to this, dithiocarbazates are among the most important hydrazinic bases because of their structural similarities to the carbazates and a considerable number of studies involving Schiff base complexes with dithiocarbazates and 2,6-diacetylpyridine have been reported [33-41].

Although Schiff bases and their metal complexes derived from dithiocarbazates with diacetylpyridine have been reported, the corresponding oxygen analogues, namely the carbazates in general and benzyl carbazate in particular, have not been previously reported. As part of our work focuses on Schiff base metal complexes derived from benzyl carbazate, we report here the synthesis of 2,6-diacetylpyridine bis(benzyl carbazate) and the template synthesis and structural characterization of its complexes with Mn(II), Fe(II), Co(II), Ni(II) or Zn(II). The thermal stability of each of these complexes is also discussed.

## 2. Experimental

### *2.1. Materials*

Benzyl carbazate and 2,6-diacetylpyridine was purchased from Sigma-Aldrich. All other chemicals and solvents were obtained from a commercial source and were used as received without further purification.

### *2.2. Synthesis of the ligand*

0.166 g (1 mmol) of benzyl carbazate and 0.082 g (0.5 mmol) of 2,6-diacetylpyridine were combined in 20 mL of methanol. Slow evaporation of the solvent from the mixture at room temperature resulted in a white crystalline precipitate which was isolated and washed with doubly- distilled water.

Ligand **$bc_2$-dap**: Colorless, 80 % yield with respect to the amount of base (benzyl carbazate) taken. Anal. Calcd for $C_{25}H_{25}N_5O_4$: C, 65.36; H, 3.96; N, 15.25%. Found: C, 65.15; H, 3.40; N, 14.95%. IR ($cm^{-1}$): 3246, 1694, 1573, 1038. $^1$H NMR (400 MHz, DMSO-$d_6$): δ 10.55 (s, 1H), 10.44 (s, 1H), 7.82-8.22 (m, 3H), 7.33-7.46 (m, 10H), 5.24 (s, 2H), 5.23 (s, 2H), 2.39 (s, 3H), 2.35 (s, 3H).

### *2.3. Synthesis of the complexes*

#### *2.3.1. [M(NCS)$_2$($bc_2$-dap)].n$H_2O$; M = Mn **(1)**, Fe **(2)**, Co **(3)**, Zn **(4)** or Co **(5)**; n=0 **(1- 4)** and n=1 **(5)***

Benzyl carbazate (0.166 g, 1 mmol) was dissolved in 10 mL of a propanol solution of 2,6-diacetylpyridine (0.082 g, 0.5 mmol). To this solution the various metal nitrates ($M(NO_3)_2.6H_2O$, (Mn=0.144 g, Co=0.146 g, Zn=0.149 g), 0.5 mmol; $Fe(NO_3)_3.9H_2O$, 0.202 g, 0.5 mmol) were added together with ammonium thiocyanate (0.076 g, 1 mmol) dissolved in 10 mL of doubly-distilled water. The resulting mixture was kept at room temperature for

crystallization. After two days, the manganese, **1**, iron, **2**, and zinc, **4**, complexes were obtained as crystalline solids. In the case of cobalt, both red, **3**, and orange, **5**, crystals were observed in the solution after two days and were isolated by filtration. These crystals were separated manually and used for further analysis.

Compound **1**: Lemon yellow, 75 % yield with respect to the amount of metal salt taken. Anal. Calcd for $C_{27}H_{25}N_7O_4S_2Mn$: Mn, 8.71; C, 51.38; H, 3.96; N, 15.54; S, 10.15%. Found: Mn, 8.25; C, 50.10; H, 3.20; N, 14.95; S, 10.05%. IR ($cm^{-1}$): 3153, 2080, 2005, 1678, 1525, 1047.

Compound **2**: Brown, 78 % yield with respect to the amount of metal salt taken. Anal. Calcd for $C_{27}H_{25}N_7O_4S_2Fe$: Fe, 8.85; C, 51.36; H, 3.96; N, 15.53; S, 10.15%. Found: Fe, 8.30; C, 51.10; H, 3.40; N, 15.30; S, 9.95 %. IR ($cm^{-1}$): 3140, 2087, 2009, 1676, 1525, 1047.

Compound **3**: Red, 20 % yield with respect to the amount of metal salt taken. Anal. Calcd for $C_{27}H_{25}N_7O_4S_2Co$: Co, 8.50; C, 51.06; H, 3.94; N, 15.44; S, 10.09%. Found: Co, 8.30; C, 51.05; H, 3.50; N, 15.10; S, 10.25 %. IR ($cm^{-1}$): 3141, 2098, 2011, 1680, 1528, 1052.

Compound **4**: Light yellow, 70 % yield with respect to the amount of metal salt taken. Anal. Calcd for $C_{54}H_{50}N_{14}O_8S_4Zn_2$: Zn, 10.20; C, 50.54; H, 3.90; N, 15.29; S, 9.98%. Found: Zn, 10.10; C, 50.00; H, 3.30; N, 15.25; S, 9.10%. IR ($cm^{-1}$): 3183, 2097, 2009, 1695, 1521, 1045. $^1$H NMR (400 MHz, DMSO-$d_6$): δ 12.48 (s, 1H), 10.47 (s, 1H), 8.08-8.14 (m, 3H), 7.43-7.97 (m, 10H), 5.48 (s, 2H), 5.24 (s, 2H), 2.50 (s, 3H), 2.37 (s, 3H).

Compound **5**: Orange, 65 % yield with respect to the amount of metal salt taken. Anal. Calcd for $C_{27}H_{27}N_7O_5S_2Co$: Co, 8.26; C, 49.65; H, 4.14; N, 15.02; S, 9.81%. Found: Co, 8.10; C, 49.30; H, 4.05; N, 14.50; S, 9.55%. IR ($cm^{-1}$): 3418, 3115, 2103, 1686, 1546, 1052. $^1$H NMR (400 MHz, DMSO-$d_6$): δ 13.60 (s, 2H), 10.28 (s, 1H), 10.50 (s, 1H), 7.97-8.56 (m, 3H), 7.35-7.66 (m, 10H), 5.25 (s, 2H), 5.20 (s, 2H), 2.48 (s, 3H), 2.36 (s, 3H).

*2.3.2. [Fe(bc-dap)($H_2O$)$_2$]. 2Cl. 4$H_2O$ **(6)***

To a methanol solution (10 mL) of benzyl carbazate (0.166 g, 1 mmol) and 2,6-diacetylpyridine (0.082 g, 0.5 mmol), an aqueous solution (10 mL) of iron(II) chloride hydrate (0.072 g, 0.5 mmol) was added drop wise. The resulting solution was allowed to slowly evaporate at room temperature. X-ray quality brown colored crystals were isolated from mother-liquor, washed with doubly-distilled water and air dried.

Compound **6**: Brown, 73 % yield with respect to the amount of metal salt taken. Anal. Calcd for $C_{25}H_{35}N_5O_{10}Cl_2Fe$: Fe, 8.85; C, 43.33; H, 5.06; N, 10.11 %. Found: Fe, 8.30; C, 43.05; H, 4.70; N, 10.20 %. IR (cm$^{-1}$): 3596, 3141, 1668, 1538, 1061. $^1$H NMR (400 MHz, DMSO-$d_6$): δ 10.42 (s, 1H), 7.35-7.88 (m, 3H), 6.42-6.66 (m, 10H), 5.15 (s, 2H), 2.47 (s, 3H), 2.27 (s, 3H).

*2.3.3. [Ni(NCS)$_2$($bc_2$-dap)]. $CH_3OH$ **(7)***

A mixture of nickel(II) nitrate hexahydrate (0.146 g, 0.5 mmol) and ammonium thiocyanate (0.076 g, 1 mmol) dissolved in doubly-distilled water (10 mL) was mixed with a methanol solution (10 mL) of benzyl carbazate (0.166 g, 1 mmol) and 2,6-diacetylpyridine (0.163 g, 1 mmol). The solution was left to stand overnight and the resulting light green crystalline compound was filtered off, washed with distilled water and air dried.

Compound **7**: Green, 73 % yield with respect to the amount of metal salt taken. Anal. Calcd for $C_{28}H_{29}N_7O_5S_2Ni$: Ni, 8.81; C, 50.42; H, 4.35; N, 14.71; S, 9.60%. Found: Ni, 8.25; C, 50.20; H, 4.00; N, 14.25; S, 8.95%. IR (cm$^{-1}$): 3581, 3169, 2106, 1708, 1618, 1520, 1043. $^1$H NMR (400 MHz, DMSO-$d_6$): δ 10.41 (s, 1H), 7.79-7.91 (m, 3H), 7.29-7.40 (m, 10H), 6.78 (s, 1H), 5.16 (s, 4H), 3.17 (s, 3H), 2.49 (s, 3H), 2.28 (s, 3H).

*2.3.4. [Co(NCS)$_2$(bc-dap)]* ***(8)***

To a 10 mL propanol solution of benzyl carbazate (0.083 g, 0.5 mmol) and 2,6-diacetylpyridine (0.082 g, 0.5 mmol), a 10 mL aqueous solution containing cobalt(II) nitrate hexahydrate(0.146 g, 0.5 mmol), zinc(II) nitrate heptahydrate (0.149 g, 0.5 mmol) and ammonium thiocyanate (0.076 g, 1 mmol) was added slowly with constant stirring. The resulting orange solution was kept at room temperature for slow evaporation of the solvent. X-ray quality green crystals of **8** were obtained after two days and separated as before.

Compound **8**: Dark green, 72 % yield with respect to the amount of metal salt taken. Anal. Calcd for $C_{17}H_{14}N_5O_2S_2Co$: Co, 13.30; C, 46.06; H, 3.16; N, 15.80; S, 14.45%. Found: Co, 13.10; C, 45.90; H, 3.05; N, 15.45; S, 14.10%. IR ($cm^{-1}$): 3068, 2091, 1734, 1694, 1518, 1053. $^1$H NMR (400 MHz, DMSO-$d_6$): δ 10.57 (s, 1H), 7.91-8.22 (m, 3H), 7.33-7.46 (m, 5H), 5.23 (s, 2H), 2.50 (s, 3H), 2.38 (s, 3H).

*2.4. Physical measurements*

The metal content in all the complexes was determined volumetrically by EDTA titration [42]. Elemental analyses for C, H, N and S were performed on a Vario-ELIII elemental analyzer. The FT-IR spectra were recorded on a JASCO-4100 spectrophotometer as KBr pellets in the range of 4,000-400 $cm^{-1}$. $^1$H NMR spectra were recorded on a Bruker Ultrashield 400 MHz ($^1$H) spectrometer using tetramethylsilane (TMS) as an internal reference. Chemical shifts are expressed in parts per million (ppm). Electronic absorption spectra were measured on a JASCO V-630 UV-vis spectrophotometer. The simultaneous TG-DTA studies were undertaken on a PerkinElmer SII Thermal Analyzer, and the thermograms were obtained in air using platinum cups as sample holders with 5-10 mg of each sample at a heating rate of 10 °C $min^{-1}$.

*2.5. X-ray crystallography*

Crystallographic data for **1**-**5** are detailed in Table 1 with those for **6**-**8** in Table 2. All X-ray measurements were performed on an Agilent SuperNova, Dual, Cu at zero, Atlas diffractometer using a mirror monochromator and Cu-K$\alpha$ radiation ($\lambda$ = 1.5418 Å) for the structures of **1**-**4**, **7** and **8** with Mo-K$\alpha$ radiation ($\lambda$ = 0.71073 Å) providing better data for the structures of **5** and **6**. All data were collected at 100(2) K. The data collection, cell refinement, data reduction and absorption corrections were applied using CrysAlisPro [43].

The structures of **1**, **2**, **6** and **8** were solved with *SHELXT* [44] and those of **3**, **4**, **5**, and **7** with *SHELXS97* [45] and refined by full-matrix least-squares on $F^2$ using *SHELXL-2014/7* [46] and *TITAN2000* [47]. All non-hydrogen atoms were assigned anisotropic displacement parameters. The H atoms on N3 and N3' in all of the complexes were located in a difference Fourier and their coordinates were refined with $U_{eq}$ = 1.2$U_{eq}$ (N). All H-atoms bound to carbon were refined using a riding model with d(C-H) = 0.95 Å, $U_{iso}$ =1.2$U_{eq}$ (C) for aromatic, 0.99 Å, $U_{iso}$ =1.2$U_{eq}$ (C) for methylene and 0.98 Å, $U_{iso}$ =1.5$U_{eq}$ (C) for the $CH_3$ H atoms. When all of the non-hydrogen atoms had been found in the structures of complexes **5** and **6** additional high peaks were found in the difference Fourier maps that could be refined as the O atoms of solvent water molecules; one for **5** and four for **6**. For **6**, one of these O atoms lies on a mirror plane. The H atoms of these solvent water molecules were all found in subsequent Fourier maps and their coordinates were refined with $U_{eq}$ = 1.5$U_{eq}$(O). For **7**, two additional high peaks appeared that were found to be from a methanol solvate molecule. The H atoms for this solvent were treated as riding for the methyl group while the coordinates of the OH hydrogen atom were refined. Crystals of **2** were of particularly poor quality. Despite collecting data on several different samples and with both Cu and Mo radiation the results presented here detail the best that could

be obtained. However, despite the poor final residuals, the structure solved and refined satisfactorily and the poor data is reflected in the uncertainties of all the parameters reported for this structure. All molecular plots and packing diagrams were drawn using *Mercury* [48]. Other calculations were performed using *PLATON* [49] and tabular material was produced using *WINGX* [50].

**3. Results and Discussion**

The ligand (**$bc_2$-dap**) can be readily prepared in good yield by the reaction of 2,6-diacetylpyridine (dap) with benzyl carbazate (bc) in methanol (Scheme 1). However, the reaction of an aqueous methanolic solution of a metal salt in presence of ammonium thiocyanate with **$bc_2$-dap** in 1:2:1 molar proportions did not yield any one of the desired complexes in stable and crystalline forms. Therefore, the synthesis of complexes of this ligand was achieved by a template method.

One-step synthesis of Schiff base complexes through a template condensation between diacetylpyridine and benzyl carbazate in the presence of various metal salts and ammonium thiocyanate at room temperature yielded a number of products, Scheme 2. Reaction of the ligand generated in-situ in the presence of the metal salts is very interesting as, depending on the metal and its associated counter anion, the reaction conditions and the solvents used in the preparation, three different types of metal complexes were obtained as homogeneous crystalline solids (Scheme 2).

In the first type, I(a), **$bc_2$-dap** acts as a pentadentate ligand and forms isotypic crystalline complexes with Mn(II), Fe(II), Co(II) or Zn(II) labelled as compounds **1-4** respectively. In each the metals are seven coordinate binding to the multidentate ligand through the carbonyl oxygens, azomethine nitrogen atoms and the pyridine nitrogen. The remaining two sites are occupied by

nitrogen atoms of anionic thiocyanato ligands that ensure the neutrality of the complexes. Closely related to these products is the Co(II) complex **5**, with comparable coordination geometry but which crystallises with a solvate water molecule. Type I(b) is represented by the Fe(II) complex **6**, the only cationic complex reported here, all the others being neutral. The coordination geometry is similar to that of **1-5** except that neutral water molecule replaces the thiocyanato ligands with two uncoordinated chloride anions for neutrality. This complex co-crystallizes with four solvent water molecules. A stable product of this type could only be obtained with iron and no comparable cationic complexes could not be isolated with other metal ions.

In the type II nickel compound, the **$bc_2$-dap** ligand formed in-situ is tetratendate coordinating to Ni(II) through the pyridyl nitrogen, both azomethine nitrogen atoms but only one of the carbonyl oxygen atoms. In attempts to prepare **7**, if the nickel nitrate, ammonium thiocyanate, benzyl carbazate and 2,6-diacetylpyridine mole ratio was 1:2:2:1, as was used for the preparation of **1-6**, the resulting product was polycrystalline in nature. Although analysis of this polycrystalline solid was consistent with the formula $C_{28}H_{29}N_7NiO_5S_2$, X-ray quality crystals could not be obtained. However, the reaction was carried out in the mole ratio 1:2:2:2, a crystalline form of compound **7** formed that was suitable for single crystal X-ray diffraction.

The third type of complex **8** is formed for Co(II) from an alternative ligand formed in-situ. Here only one benzyl carbazate has condensed with the diacetyl pyridine to produce the mono-Schiff base (bc-dap). A notable feature of this type III complex is that the Co(II) cation is tetrahedrally coordinated, binding to the pyridine and azomethine N atoms of the bidentate **bc-dap** ligand. Two N-bound thiocyanato ligands complete the tetrahedral coordination sphere of the neutral complex. This compound was obtained as an unintentional product of an attempt to

prepare mixed metal complexes of cobalt and zinc; green crystals of the Co(II) compound appeared floating in the mother liquor in very low yield. Reaction of metal salts (cobalt and zinc nitrates), ammonium thiocyanate, benzyl carbazate and 2,6-diacetylpyridine in the mole ratio of ½:½:2:2:1 resulted in the 1:2:1:1 product with low yield.

Analytical results confirmed the proposed composition (1:2:1:1). Once the structure of this complex was determined crystallographically, the reaction was repeated with the mole ratio ½:½:2:1:1 (Co:Zn:$NH_4SCN$:bc:dap) that gave the green product in greater yield. It is interesting to note here that, attempts to synthesize complex **8** without zinc nitrate present in the reaction mixture were entirely unsuccessful. However, the same reaction carried out with other metal ions instead of zinc did not yield any tractable products. The role of the zinc ion, in this reaction is not clear at present.

However, the present Schiff base, irrespective nature of the metal salt used, yielded complexes containing only the protonated form of the ligand. The result of these reactions depends on the nature of the ligands, as well as on the coordination preferences of the metal ions. Efforts to prepare the analogous chromium and copper complexes were unsuccessful, probably due to the reducing nature of these metal ions. All the complexes that were obtained are stable in air and insensitive to light. They are insoluble in water, methanol and ethanol, and soluble in DMSO.

*3.1. Infrared spectra*

The infrared spectra of the ligand (**$bc_2$-dap**) and complexes (**1-8**) were recorded to confirm their structures and the IR spectra of ligand (**$bc_2$-dap**) and complexes (**3** & **5-8**) are shown in Fig. S1-S6 as representative examples. The main IR bands of the ligand are found at 1694 and 1573 $cm^{-1}$ and may be assigned to C=O and C=N stretching vibrations, respectively.

These bands undergo shifts of 8-26 $cm^{-1}$ and 27-53 $cm^{-1}$, respectively, to lower wavenumbers for the complexes (**1-6**) upon binding the ligand to the central metal ion through the oxygen atoms of both carbonyl groups and both azomethine nitrogen atoms. Shifts to lower wavenumber on binding the azomethine N atom of a Schiff base to a metal atom has been observed previously [39]. Also a shift of the C=O stretching vibration to lower frequency on coordination to a metal is a common observation [51]. Unlike the other compounds, complex **7** displayed a sharp peaks at 1708 and 1618 $cm^{-1}$ corresponding to the C=O stretching frequency of an uncoordinated and coordinated carbonyl groups respectively. Complex **8** showed two discrete C=O stretching modes at 1736 $cm^{-1}$ due to the C=O stretching of carbonyl group of the diacetylpyridine and at 1695 $cm^{-1}$ from the amide C=O of benzyl carbazate. Further, evidence of coordination of **$bc_2$-dap** to the metal ion through the azomethine nitrogen atom comes from the shift of the N-N stretching of the free ligand (1028 $cm^{-1}$) to higher wave numbers in the spectra of the complexes (to ~1050 $cm^{-1}$ in most cases) [52]. Coordination via the pyridine nitrogen atom is also indicated by the out-of-plane ring deformation at 600 $cm^{-1}$ shifting to higher energies by 20 $cm^{-1}$ [53]. The presence of both coordinated and solvent water molecules in **6** is indicated by the appearance of O-H bands at 3141 and 3596 $cm^{-1}$. Bands at 3418 and 3580 $cm^{-1}$ in complexes **5** and **7** have been assigned to the O-H stretching frequencies of the uncoordinated solvent water and methanol molecules. The IR spectra of the compounds (**1-4**) display a noticeable difference in the $\nu_{CN}$ band of $SCN^-$, showing two bands around 2080 and 2010 $cm^{-1}$, whereas, there is only one band at 2100 $cm^{-1}$ in compounds **5**, **7** and **8**. Despite the superficial similarity between the isotypic structures **1**-**4** and the similarly constructed hydrated complex **5**, the M-N4-C16 angles in **1**-**4** differ by close to 50˚ whereas the difference for **5** is only approximately 12˚. Hence the variation in the number of C≡N stretching modes between **1**-**4** and **5** is not surprising [54]. In **7** and **8**, the

environments of the thiocyanate ligands are also reasonably similar suggesting a rationale for the observation of a single stretching mode in each case.

*3.2. $^1$H NMR spectra*

The $^1$H NMR spectra of the free ligand (**bc$_2$-dap**) and complexes **4-8** were recorded in DMSO-d$_6$ as typical examples. The assignments of the main signals in the $^1$H NMR spectra are reported in the experimental section and the spectra are shown in figures in the supplementary material (Fig. S7-S12). The spectrum of the ligand (**bc$_2$-dap**) exhibits signals at 2.35 and 5.23 ppm corresponding to the $CH_3$ and $OCH_2$ protons, respectively. Signals due to the aromatic hydrogens of the phenyl rings appear within the range of 7.33-7.46 ppm while the heteroaromatic protons of pyridine ring appeared as multiplets in the range 7.82-8.22 ppm. The singlets at 10.44 and 10.55 ppm are ascribed to the hydrazinic NH proton of the carbazate moieties. The signals corresponding to these protons, in the spectra of complexes (**4-8**), are observed in the range 2.28-2.67, 5.15-5.48, 6.42-7.66, 7.35-8.55 and 10.41-12.48 ppm, respectively. All proton resonances found for the free ligand were also seen, albeit with some chemical shift differences, in the spectra of the complexes suggesting that no deprotonation of the ligand occurred during complex formation. Apart from these signals, the singlet at 1.24 ppm corresponds to the water molecule in complex **5**. Further, the $^1$H NMR spectrum of complex **5** shows a broad peak at chemical shift δ 13.60 for the enolic OH protons, indicating that in solution, the ligand exists in keto-enol tautomeric forms. The protons of water molecules in **6** appear as a broad signal at 1.27 ppm corresponding to both lattice and coordinated water molecules. A sharp peak at 3.17 ppm and a broad signal at 6.78 ppm for **7** are those $OCH_3$ and OH groups of the methanol solvent molecule. Thus, NMR studies support the conclusions drawn from the infrared spectra about the bonding mode of the Schiff bases.

*3.3. Electronic spectra*

The electronic spectra of the complexes were recorded in DMSO and the spectra are shown in Fig. S13-S18. The manganese **1** and zinc **4** complexes show no prominent absorption in the visible region because Mn(II) with a high-spin $d^5$ electronic configuration has no spin-allowed d-d transition and Zn(II) with a $d^{10}$ configuration also lacks d-d transitions [55]. The intense band at 536 and 548 nm for iron complexes **2** and **6**, respectively are attributed to ligand charge transfer transitions for Fe(II) [56]. The d-d band cannot be observed as it is obscured by a strong charge transfer transition in each case [53]. The absorption bands at 624 and 626 nm for the cobalt complexes **3** and **5**, respectively can be attributed to d-d transition [21] and support the seven-coordinated pentagonalbipyramidal geometry around cobalt(II) ions with the $CoN_5O_2$ chromophoric group. The electronic spectrum of nickel compound **7** shows three bands at 400, 659 and 745 nm corresponding to the $^3A_{2g}$ (F) $\longrightarrow$ $^3T_{2g}$ (F), $^3A_{2g}$ (F) $\longrightarrow$ $^3T_{2g}$ (F) and $^3A_{2g}$ (F) $\longrightarrow$ $^3T_{1g}$ (P) transitions respectively, confirming an octahedral geometry around the metal ion [57]. A broad band at 606 nm may be assigned to $^4A_2$(F) $\longrightarrow$ $^4T_1$(P) transition for Co(II) ion in a tetrahedral coordination environment found in **8** [24].

*3.4. Crystal structures*

*3.4.1. Molecular structures of **1-5***

The molecular structures of **1-5** and their atom numbering schemes are shown in Fig.1. Crystallographic data and structure refinement parameters are summarized in Table 1 and selected bond distances and angles are given in Tables S1 and S2. Compounds **1- 4** are isotypic; all four complexes have similar coordination spheres with the metal centres coordinated by the pyridine nitrogen and two azomethine nitrogen atoms together with the two carbonyl oxygen atoms of the pentadentate ligands. These complexes display the same coordination geometry and

all of them crystallize in the monoclinic space group $P2_1/n$. Complex **5** is closely similar to compounds **1**-**4** but, interestingly, **5** crystallizes as a monohydrate with a completely different unit cell and crystal packing. All five complexes are monomeric and the metal ions are in seven coordinate pentagonal bipyramidal environments. The two nitrogen atoms from the thiocyanato anions are found in apical positions and the planar pentadentate ONNNO coordinated **bc$_2$-dap** ligands each bind through the carbonyl oxygen atoms, the two azomethine nitrogen atoms and the pyridine nitrogen atom to form the equatorial plane. The coordinated Schiff base ligand presents an almost ideal pentagonal array of donor atoms (Fig. 2). Four of the angles subtended at the metal atom by adjacent equatorial atoms vary only slightly than the value of 72˚ expected for an ideal pentagonal bipyramidal arrangement, ranging from 68-71˚. In contrast the O8-M-O8' angles are consistently wider across the series and their range of values is also much greater ranging from 85-76˚, Table S1. An interesting structural feature of **1-5** is that the M-O bond lengths are consistently longer than the M-N bond distances (Table S1).

A striking feature of the coordination of the two *trans*-axial thiocyanato ligands is the sharp contrast between the values of the C16-N4-M and C16'-N4'-M angles in all four structures, Table S2. The C16'-N4'-M angles do not differ severely from the ideal 180˚, (range 173.97(13)-169.1(8)) such that the S1'-C16'-N4'-M is reasonably linear, the corresponding range of C16-N4-M angles is 125.3(7)-122.82(14) such that there is a significant bend at the N4 atom in each case, widening the angle between the $SCN^-$ and the *trans* axial line by up to 40˚. Similar significant variations from linearity in the placement of thiocyanato ligands have been observed in one polymorph of the complex $[Co(SCN)_4(ppz\text{-}H)_2]$ (ppz = piperazine) [54]. As mentioned previously, this is likely to be the reason for the occurrence of two $\nu_{CN}$ strethching modes in the infrared spectra. In an interesting contrast, the bending at N4 and N4' for the hydrated analogue **5**

is less severe and almost equivalent for each of the thiocyanato ligands with C16-N4-Co1 = 150.22(15) and C16'-N4'-Co1 = 161.97(16).

As expected for isostructural systems of **1**- **4**, the packing features of these complexes are almost identical therefore the packing of compound **4** is used as a representative example. The pyridine and C10/C15 phenyl rings form an offset π…π contact with a centroid to centroid separation of 3.7831(9) Å. In addition, a C-H…π (ring) contact C71'-H71F…Cg3 also forms linking each complex molecule to others (Fig. S19a). An eclectic mix of classical N-H…N and N-H…S hydrogen bonds, Table S3, together with C-H…O and C-H…S contacts complete the three dimensional network with complexes stacked along the *b* axis direction (Fig. S19b). Packing diagrams for **1**-**3** appear in Figs. S20-S22 respectively.

Unsurprisingly, the crystal structure of the solvated complex **5** is somewhat different from those of **1**-**4** complexes despite the similarities in the structures of the complexes themselves. In particular the solvent water molecule is involved in O-H…S, N-H…O and C-H…O hydrogen bonds, Table S4. Molecules of **5** are linked into chains through the N-H…S, C-H…S and O-H…S interactions. The chains are arranged into sheets in the *bc* plane through O-H…S and C-H…N hydrogen bonds. In addition to these interactions, C-H…π combine to generate a 3-dimensional supramolecular network, Fig. S23.

*3.4.2. Molecular structure of* ***6***

Compound **6** crystallized in the monoclinic space group $P2_1/m$ with two molecules in the unit cell as the iron atom, Fe1, lies on mirror plane, Fig. 3. The O1, O2 and O2W atoms of water molecules and their associated H atoms also lie on this plane as does the O3W atom. O1W is in a general position so that four solvent water molecules in total co-crystallise with the complex

molecule. The charge on the Fe(II) complex is neutralized by two non-coordinating chloride anions. The coordination geometry about the metal centre is pentagonal bipyramidal similar to that adopted by complexes **1-5** with the neutral **bc$_2$-dap** ligand coordinating through its carbonyl oxygen azomethine nitrogen and pyridine nitrogen atoms and forming the basal (pentagonal) plane. Two coordinated water molecules occupy axial positions and complete the coordination sphere. Selected bond distances and angles are detailed in Table S5. Unlike the situation for **1**-**5** where the M-N$_{py}$ and M-N$_{azo}$ distances were reasonably similar for a given complex, here Fe-N1$_{py}$ at 2.205(5) Å is shorter than Fe-N2$_{azo}$, 2.229(3) Å, with Fe-O8 = 2.236(3) Å. The Schiff base ligand again adopts almost ideal pentagonal geometry with the N-Fe-N and O-Fe-N angles close to the ideal 72˚. As was found in complexes **1-5**, the O-Fe-O angle is much wider, Fig. S24.

Packing in this structure is achieved through an extensive range of intermolecular interactions, Table S6. Interestingly, there are no direct contacts between the complex cations; the lattice chloride anions and water molecules act as donors and acceptors to bridge neighboring cationic units. The cations are linked into a one-dimensional chain along the *c* axis through C4-H4…O3W interactions. An extensive series of O-H…O, C-H…O, O-H…Cl and C-H...Cl hydrogen bonds join adjacent chains forming two-dimensional sheets of cations, anions and water molecules in the *bc* plane (Fig. S25a). These sheets are further interconnected by O-H…O and C-H…O hydrogen bonds involving the solvent water molecules to generate a three-dimensional network with the cations stacked along the *c* axis direction (Fig. S25b).

*3.4.3. Molecular structure of **7***

The asymmetric unit of the structure of **7** comprises a neutral Ni(II) complex that lies on a general position in the orthorhombic space group $P2_12_12_1$, and a methanol solvent molecule Fig. 4. Selected bond distances and angles are given in Table S7. The structure of compound **7** is type II, with highly distorted octahedral coordination around the Ni(II) cation. Unlike the previous set of complexes **1**-**6**, here the Schiff base provides only four donor atoms (N3O) from the essentially planar ligand environment that forms the equatorial plane. The fifth and sixth coordination sites of the octahedron are occupied by two nitrogen atoms of thiocyanate anions in the axial positions. Fig. 4 clearly shows that the **bc$_2$-dap** ligand came close to achieving the pentadentate coordination displayed in complexes **1**-**6** but the Ni-O8′ bond distance, 2.767(3) Å, is too great to be considered a bonding interaction. As a consequence, the octahedral coordination geometry of the molecule (Fig. 5) is severely distorted with N1-Ni1-N2, N1-Ni1-N2′ and N2′-Ni1-O8′ all very much less than the ideal 90˚ while in compensation, the O8′-Ni1-N2 angle is exceptionally large at 138.26(13)˚. The best fit plane through the four ligand donor atoms has an *rms* deviation of 0.0126 Å. With the exception of the phenyl rings, the remaining parts of the tetradentate ligands are also reasonably co-planar with an *rms* deviation 0.0976 Å for **7** from the best fit plane through the remaining 22 non-hydrogen atoms. The phenyl rings of the benzyl units subtend angles of **7**2.62(9) and 68.58(4)˚ to this plane. The bonding parameters of the terminal NCS ligands in **7** fall well within the range generally observed in the literature [58,59]. The terminal M-NCS linkages are again bent with C16-N4-Ni1 at 159.9(4)˚ more markedly so in comparison to C16'-N4'-Ni1 at 177.0(3)˚. These angles fall in the range generally found for $Ni^{2+}$ complexes with N bound $NCS^-$ ligands [60].

In the crystal packing of **7**, pairs of adjacent complex molecules are linked by C71-H71C…Cg5 hydrogen bonds, Table S8, and π…π stacking interactions (Cg4…Cg6$^{7ii}$ 3.609(3) Å, 7ii = x-1/2, -y+1/2, -z+1) to form chains of complex molecules parallel to (103), Fig. S26a. (Cg2, Cg4 and Cg6 are the centroids of the N1/C2-C6, C10-C15 and C10′-C15′ rings respectively). Classical N-H…S and non-classical C-H…S hydrogen bonds also link the complex molecules. In addition, the methanol solvate molecule forms hydrogen bonds to the complex molecules that involve all three hydrogen atoms of the methyl group, but no sensible contact from the OH group is found. This variety of contacts combine to generate and extensive three dimensional network with the complex molecules stacked along the *a* axis direction, Fig. S26b.

*3.4.4. Molecular structure of **8***

The molecular structure of the complex **8** is shown in Fig. 6 and the crystallographic information with the selected bond parameters are provided in Tables 2 and S9 respectively. In this instance the ligand that formed in-situ was a mono-Schiff base as the diacetyl substrate condensed with only one benzyl carbazate molecule resulting in the bidentate bc-dap ligand. The neutral complex **8** has a four-coordinate mononuclear cobalt(II) centre bound to the neutral bidentate **bc-dap** ligand and two $NCS^-$ anions. It is interesting to note that unlike other complexes (**1-7**), compound **8** adopts tetrahedral coordination geometry. In the former, the ligand has two Schiff base centres from the **$bc_2$-dap** ligands that can provide five donor atoms (N3O2) in a basal plane. Here however, the smaller **bc-dap** ligand, uses only two donor atoms, the pyridine nitrogen and an azomethine nitrogen atoms. The two remaining coordination sites are occupied by the nitrogen atoms of two thiocyanate anions.

Tetrahedral coordination is confirmed for the complex by calculating the $\tau_4$ index.

$$\tau_4 = [360^\circ - (\alpha + \beta)]/141^\circ$$

α and β are the two largest angles subtended by the ligand donor atoms in the four-coordinate complex. $\tau_4 = 0$ for perfect square planar and 1 for ideal tetrahedral coordination geometry [61]. The $\tau_4$ value 0.88 for **8** clearly confirms some distortion from tetrahedral coordination geometry in this case as evidenced in particular by the angles N1-Co-N2 (76.27(15)˚) and N4-Co-N5 (121.74 (19)˚) [62]. The Co-$N_{imine}$ (2.135(4)Å) and Co-$N_{pyridine}$ (2.091(4)Å) bonds are slightly longer than those to the nitrogen atoms of the thiocyanato anions (1.923(5) and 1.939(4)Å, respectively); these are comparable to those found in $(N(Me_4)_2$ $[Co(NCS)_4]$ [63]. The two SCN- ions are both almost linear (N4-C16-S1 = 176.7(5) and N5-C17-S2 = 178.9(5)˚), but a slight bending occurs for both Co-N-C(-S) linkages with Co-N-C angles (162.6(5) and 173.1(5)˚) respectively. These bond angles are comparable to those found in previously reported tetrahedral Co(II) complexes with thiocyanato ligands [64].

In the crystal structure of **8**, N3-H3N…N4 hydrogen bonds form inversion dimers and enclose $R^2_2(10)$ rings. These contacts are bolstered by π…π stacking interactions (Cg2…$Cg3^{8i}$ = 3.687 Å, Cg2 and Cg3 and are the centroids of the N1/C2…C6 and C10…C15 rings respectively) Fig. S27a. C14-H14…S1 hydrogen bonds link adjacent dimers into double chains of complex molecules along the *ac* diagonal. C4-H4…O8 hydrogen bonds combine with C71-H71B…O21 hydrogen bonds to enclose $R^2_2(14)$ rings and link the molecules into zig-zag chains along *c*. Parallel chains are linked in an obverse fashion by C-H…S hydrogen bonds with S2 acting as a bifurcated acceptor forming C3-H3…S2 and C15-H15…S2 hydrogen bonds. The C3-H3…S2 hydrogen bonds form inversion dimers and generate $R^2_2(16)$ ring motifs, Fig. S27b.

These various contacts (Table S10) combine to stack the complex molecules along the *a* axis direction, Fig. S27c.

*3.5. Thermal behavior*

To examine the thermal stability of the various complexes, simultaneous TG-DTA of the ligand (**$bc_2$-dap**) and complexes (**1-8**) have been recorded and thermograms of compounds **2**, **4, 6, 7** and **8** are shown in Fig. S28-S33 as representative examples. Thermal decomposition modes of all complexes are detailed in Table S11.

The Schiff base ligand (**$bc_2$-dap**) undergoes three decomposition steps in the TG, in accordance with the DTA results. The first peak at around 140 ˚C corresponds to melting. In the TG curve, the first mass loss (observed: 47.28 %; calculated: 47.06 %) corresponds to the loss of two benzyl alcohol molecules, which are seen as endotherms at 190 and 230 ˚C, in DTA. In the second step, the observed mass loss of 65.46 % (calc. 64.92 %) in the temperature range 250-300 ˚C corresponds to the formation of 2,6-diacetylpyridine as an intermediate. This intermediate further decomposes exothermically giving gaseous products, at 570 ˚C. Our efforts to separate and further investigate these intermediates were unsuccessful due to the continuous decomposition of the products, as evident from the TG curve. Hence, we have assigned the nature of the likely intermediate from the mass loss observed in the TG analysis (Table S11), which is consistent with the calculated mass loss.

From the thermograms (Fig. S29 & S30), it is clear that complexes **1-4** show two distinct steps of decomposition in the TG. Compounds (**1-4**) are anhydrous and start to decompose above 130 ˚C, the weight loss in the first step is due to the loss of two molecules each of benzene and carbon monoxide resulting in formic acid (1-{6-[1-(formyl-hydrazono)-ethyl]-pyridin-2-yl}-ethylidene)-hydrazidebis(N-thiocyanato)metal(II), $[M(X)(NCS)_2]$, intermediates (see the

footnote to Table S11 for the structure of X). Further, these intermediates decompose to yield the respective metal oxides as the final products. DTA shows exothermic peaks between 375 and 575 ˚C for this decomposition. Compounds **5** and **7** show three steps of decomposition in the TG. The first step corresponds to the loss of water for 5 and methanol molecules for **7**, respectively. Corresponding to this, an endotherm is observed at 105 and 90 ˚C for **5** and **7**, respectively, in the DTA. These low temperature decomposition processes are consistent with the observation that the solvent molecules are non-coordinated as found in the X-ray determinations. The remaining steps are similar to those for complexes **1-4**. After the removal of the solvent molecules, the resulting desolvated compounds decompose at a lower temperature than the previous set of complexes, as expected, due to pre heating.

Compound **6** undergoes three stages of mass loss upon heating. The first stage, which occurs in the range 10-55 ˚C, is attributed to the loss of the four solvate water molecules. In the DTA, this loss of water is observed as an endotherm around 40 ˚C and such a low temperature of dehydration again supports the presence of lattice water molecules. The anhydrous compound, then, decomposes in an endo- followed by an exothermic fashion to give a (1-{6-[1-(formyl-hydrazono)-ethyl]-pyridin-2-yl}-ethylidene)-hydrazide)iron(II) chloride, [Fe(X)].2Cl intermediate. In the final step, this intermediate decomposes exothermically to give $Fe_3O_4$ as the final residue.

In compound **8**, the endotherm at 200 ˚C of the DTA is attributed to the loss of both benzene and carbon monoxide molecules, which is supported by the weight loss in TG, to form formic acid [1-(6-acetyl-pyridin-2-yl)-ethylidene]-hydrazidebis(N-thiocyanato)cobalt(II), $[Co(Y)(NCS)_2]$ as an intermediate (see the footnote to Table S11 for the structure of Y). This intermediate further decomposes exothermically into cobalt oxide, in the range 235-625 ˚C. Our

effort to isolate the intermediates was again unsuccessful due to its continuous decomposition. Once again we have assigned the nature of the likely intermediate from the mass losses observed in the TG analysis (Table S11), which are consistent with the calculated values.

**4. Conclusion**

Our present work is focused on the design and development of new molecular coordination complexes. We have successfully synthesized three types of Schiff base complexes derived from 2,6-diacetylpyridine and benzyl carbazate by a template method under different reaction conditions. The products were characterized by various spectroscopic techniques and the solid state structures of the complexes have been determined by X-ray crystallography. From these studies, the variety of Schiff base ligands formed in-situ from 2,6-diacetylpyridine and benzyl carbazate, the complexes showed interesting and perhaps surprising structural diversity. Metal complexes **1-6** adopt pentagonal bipyramidal geometry with the same polydentate ligand environment but different central metal ions, and ancillary ligands and degrees of solvation. In **7** the Schiff base binds to the nickel ion in a tetradentate fashion with one of the carbonyl oxygens no longer coordinated. This ligand occupies the equatorial plane with thiocyanato anions in axial positions, such that the geometry around nickel is octahedral. Finally complex **8** has a simpler ligand system with a single Schiff base unit. This ligand binds to the cobalt centre as a neutral bidentate neutral chelator with the remaining sites of the tetrahedral complex occupied by thiocyanate ions. Unlike the situation found with dithiocarbazate ligands, the ligands in these complexes are invariably neutral. The pentagonalbipyramidal, octahedral and tetrahedral complexes **1-8** undergo endo-/exothermic decomposition to give complex intermediate, $[M(X)(NCS)_2]$/[Fe(X)].2Cl/$[Co(Y)(NCS)_2]$ (see

Table S11). These intermediates decompose further in an exothermic fashion to form the respective metal oxides as the final products.

**Appendix A. Supplementary data**

CCDC 1559691-1559698 contains the Supplementary crystallographic data for **1**, **2**, **6**, **5**, **7**, **3**, **8** and **4**. These data can be obtained free of charge via http://www.ccdc.cam.ac.uk/conts/retrieving.html, or from the Cambridge Crystallographic Data Centre, 12 Union Road, Cambridge CB2 1EZ, UK; fax: (+44) 1223-336-033; or e-mail: deposit@ccdc.cam.ac.uk.

**Acknowledgements**

P. Nithya acknowledges the University Grant Commission (UGC-SAP), New Delhi, India, for the award of a BSR - Senior Research Fellowship. S. Govindarajan would like to thank UGC, New Delhi, for sponsoring a UGC-Emeritus fellowship. We thank the University of Otago for the purchase of the diffractometer, and the Chemistry Department, University of Otago for the support of the work of JS.

**References**


1. T.L. Zhang, J.C. Song, J.G. Zhang, G.X. Ma, K.B. Yu , Z. Naturforsch 60b (2005) 505.
2. G. Ma, T. Zhang, K. Yu, J. Braz. Chem. Soc. 16 (2005) 796.
3. K. Srinivasan, S. Govindarajan, W.T.A. Harrison, J. Coord. Chem. 64 (2011) 3541.
4. A. Kathiresan, K. Srinivasan, S. Brinda, M. Nethaji, S. Govindarajan, Transit. Met. Chem. 37 (2012) 393.
5. K. Srinivasan, A. Kathiresan, S. Govindarajan, J.T. Aughey W.T.A. Harrison, J. Coord. Chem. 67 (2014) 857.
6. K. Srinivasan, A. Kathiresan, W.T.A. Harrison, S. Govindarajan, J. Coord. Chem. 67 (2014) 3324.
7. C. Sitong, G. Weiming, Z. Bo, Z. Tonglai, Y. Li, Polyhedron 117 (2016) 110.
8. S-T Chen, W-M Guo, T-L Zhang, J. Coord. Chem. 69 (2016) 2610.
9. L.M. Sousa, P.P. Corbi, A.L.B. Formiga, M. Lancellotti, I.M. Marzano, E.C. Pereira-Maia, G. Von Poelhsitz, W. Guerra, J. Mol. Struct. 1097 (2015) 15.
10. M.A. Rodrigues, I.M. Marzano, G.H. Ribeiro, L.C. Vegas, M. Pivatto, A.P.S. Fontes, C.M. Ribeiro, F.R. Pavan, K.J. de Almeida, A.A. Batista, E.C. Pereira-Maia, W. Guerra, Polyhedron 98 (2015) 146.
11. P. Nithya, J. Simpson, S. Helena, R. Rajamanikandan, S. Govindarajan, J. Therm. Anal. Calorim. 129 (2017) 1001.
12. P. Nithya, S. Helena, J. Simpson, M. Ilanchelian, A. Muthusankar, S. Govindarajan, J. Photochem. Photobiol. B 165 (2016) 220.
13. P. Nithya, J. Simpson, S. Govindarajan, Inorg. Chim. Acta 467 (2017) 180.
14. W.R. Paryzek, M. Gdaniec, Polyhedron 16 (1997) 3681.

15. A.D. Azaz, S. Celen, H. Namli, O. Turhan, R. Kurtaran, C. Kazak, N.B. Arslan, Transit. Met. Chem. 32 (2007) 884.

16. C. Kazak, N.B. Arslan, S. Karabulut, A.D. Azaz, H. Namlı, R. Kurtaran, J. Coord. Chem. 62 (2009) 2966.

17. N.K. Shee, S. Dutta, M.G.B. Drew, D. Datta, Inorg. Chim. Acta 398 (2013) 132.

18. A.J. Osinski, B.A. Hough, L.A. Crandall, I.S. Tamgho, C.J. Ziegler, Inorg. Chem. Communi. 59 (2015) 76.

19. S. Chandra, A.K. Sharma, Spectrochim. Acta Part A 72 (2009) 851.

20. S. Chandra, A.K. Sharma, J. Coord. Chem. 62 (2009) 3688.

21. S. Konar, A. Jana, K. Das, S. Ray, S. Chatterjee, J.A. Golen, A.L. Rheingold, S.K. Kar, Polyhedron 30 (2011) 2801.

22. A.K. Sharma, S. Chandra, Spectrochim. Acta Part A 78 (2011) 337.

23. P. Bourosh, I. Bulhac, A. Mirzac, S. Shova, O. Danilescu, Russ. J. Coord. Chem. 42 (2016) 157.

24. A.A.A. Abu-Hussen, W. Linert, Spectrochim. Acta Part A 74 (2009) 214.

25. G. Hu, H. Miao, H. Mei, S. Zhou, Y. Xu, Dalton Trans. 45 (2016) 7947.

26. M.C. Rodriguez-Argiielles, M.B. Ferrari, G.G. Fava, C. Pelizzi, P. Tarasconi, R. Albertini, P.P. Dall'Aglio, P. Lunghi, S. Pinelli, J. Inorg. Biochem. 58 (1995) 157.

27. J.S. Casas, E.E. Castellano, M.S. Garcia-Tasende, A. Sfinchez, J. Sordo, M.J. Vidarte, Polyhedron 17 (1998) 2249.

28. R. Pedrido, M.R. Bermejo, M. J. Romero, M. V´azquez, A.M. Gonz´alez-Noya, M. Maneiro, M.J. Rodr´ıguezb, M.I. Fern´andez, Dalton Trans. (2005) 572.

29. A. Panja, C. Campana, C. Leavitt, M.J. Van Stipdonk, D.M. Eichhorn, Inorg. Chim. Acta 362 (2009) 1348.

30. Y.S. Rao, B. Prathima, S. Adinarayana Reddy, K. Madhavic, A. Varada Reddy, J. Chin. Chem. Soc. 57 (2010) 677.

31. A.I. Matesanz, P. Souza, Inorg. Chem. Communi. 27 (2013) 5.

32. A.I. Matesanz, C. Hernandez, J. Perles, P. Souza, J. Organomet. Chem. 804 (2016) 13.

33. M. Akbar Ali, A.H. Mirza, A.L. Tan, L.K. Wei, P.V. Bernhardt, Polyhedron 23 (2004) 2037.

34. G.F. de Sousa, J.V. Martı´nez, S.H. Ortega, Acta Crystallogr. E61 (2005) m1810.

35. G.F. de Sousa, V.A. da S. Falcomer, Y.P. Mascarenhas, J. Ellena,Jose´ D. Ardisson, J.V. Martı´nes, S.H. Ortega, Transit. Met. Chem. 31 (2006) 753.

36. M.A. Ali, A.H. Mirza, L.K. Wei, P.V. Bernhardt, O. Atchade, X. Song, G. Eng, L. May, J. Coord. Chem. 63 (2010) 1194.

37. M.A. Ali, A.H. Mirza, S.T. Wai Keng, R.J. Butcher, Transit. Met. Chem. 28 (2003) 241.

38. M.A. Ali, A.H. Mirza, R.J. Butcher, K.A. Crouse, Transit. Met. Chem. 31 (2006) 79.

39. M.A. Ali, A.H. Mirza, C.W. Voo, A.L. Tan, P.V. Bernhardt, Polyhedron 22 (2003) 3433.

40. A.H. Mirza, M.A. Ali, P.V. Bernhardt, I. Asri, Polyhedron 81 (2014) 723.

41. M.A. Ali, A.H. Mirza, R.J. Butcher, M.T.H. Tarafder, M.A. Ali, Inorg. Chim. Acta 320 (2001) 1.

42. Vogel AI (1961) A textbook of quantitative inorganic analysis including elementary instrumental analysis, 3rd ed. Longman, London

43. Agilent (2014) CrysAlispro. Agilent Technologies, Yarnton, Oxfordshire, England.

44. G.M. Sheldrick, Acta Crystallogr. A71 (2015) 3.

45. G.M. Sheldrick, Acta Crystallogr. A64 (2008) 112.

46. G.M. Sheldrick, Acta Crystallogr. C71 (2015) 3.

47. K.A. Hunter, J. Simpson, TITAN2000. (1999) University of Otago, New Zealand

48. C.F. Macrae, I.J. Bruno, J.A. Chisholm, P.R. Edgington, P. Mccabe, E. Pidcock, L.R. Monge, R. Taylor, J. van de Streek, P.A. Wood, J. Appl. Crystallogr. 41 (2008) 466.

49. A.L. Spek, Acta Crystallogr. D65 (2009) 148.

50. L.J. Farrugia, J. Appl. Cryst. 45 (2012) 849.

51. K. Nakamoto, (2009) Infrared and Raman spectra of inorganic and coordination compounds, Sixth Edition. Wiley. Hoboken, New Jersey.

52. R. Ugo, J. Organomet. Chem. 9 (1967) 395.

53. C.A. Brown, D.X. West, Transit. Met. Chem. 28 (2003) 154.

54. S.C. Manna, A.D. Jana, M.G.B. Drew, G. Mostafa, N.R. Chaudhuri, Polyhedron 27 (2008) 1280.

55. M. Yamami, M. Tanaka, H. Sakiyama, T. Koga, K. Kobayashi, H. Miyasaka, M. Ohba, H. Okawa, J. Chem. Soc. Dalton Trans, 1997, 4595.

56. S.Y. Shaban, M.M. Ibrahim, F.W. Heinemann, R.V. Eldik, J. Coord. Chem 65 (2012) 934.

57. B. Lefez, P. Nikeng, J. Lopitaux and G. Poillerat, Mat. Res. Bull. 31 (1996) 1263.

58. R. Kapoor, A. Kataria, A. Pathak, P. Venugopalan, G. Hundal, P. Kapoor, Polyhedron 24 (2005) 1221.

59. L. Pauling, The Nature of Chemical Bond, Cornell University Press, Ithaca, NY, (1960)

60. T.L. Borgne, J.M. Benech, S. Floquet, G. Bernardinelli, C. Aliprandini, P. Bettens, C. Piguet, J. Chem. Soc., Dalton Trans. (2003) 3856.

61. L. Yang, D.R. Powell, R.P. Houser, Dalton Trans. (2007) 955.

62. S. Sabiah, B. Varghese, N.N. Murthy, J. Chem. Crystallogr. 40 (2010) 1195.

63. E. Shurdha, C.E. Moore, A.L. Rheingold, S.H. Lapidus, P.W. Stephens, A.M. Arif, J.S. Miller, Inorg. Chem. 52 (2013) 10583.

64. B. Machura, J. Palion, M. Penkala, T. Gron, H. Duda, R. Kruszynski, Polyhedron 56 (2013) 189.

**Figures:**

**Scheme 1**

Synthesis of the ligand **$bc_2$-dap**

**Scheme 2**

Synthetic routes for the preparation of complexes (**1-8**)

**Fig. 1**

The molecular structures of **1**-**4** (**a-d**) and the asymmetric unit of **5** (**e**) with ellipsoids drawn at the 50 % probability level

**Fig. 2**

A representative view of the coordination environment in **1**-**5** as illustrated by compound **4**

**Fig. 3**

The asymmetric unit showing the complex molecule, counter ion and solvate molecules of **6** showing the atom numbering. Numbered atoms are related to unnumbered atoms by the symmetry operation x, -y+3/2, z. Ellipsoids are drawn at the 50 % probability level.

**Fig. 4**

The asymmetric unit of **7** with ellipsoids drawn at the 50% probability level

**Fig. 5**

The coordination environment of **7**

**Fig. 6**

The molecular structure of **8** with ellipsoids drawn at the 50% probability level

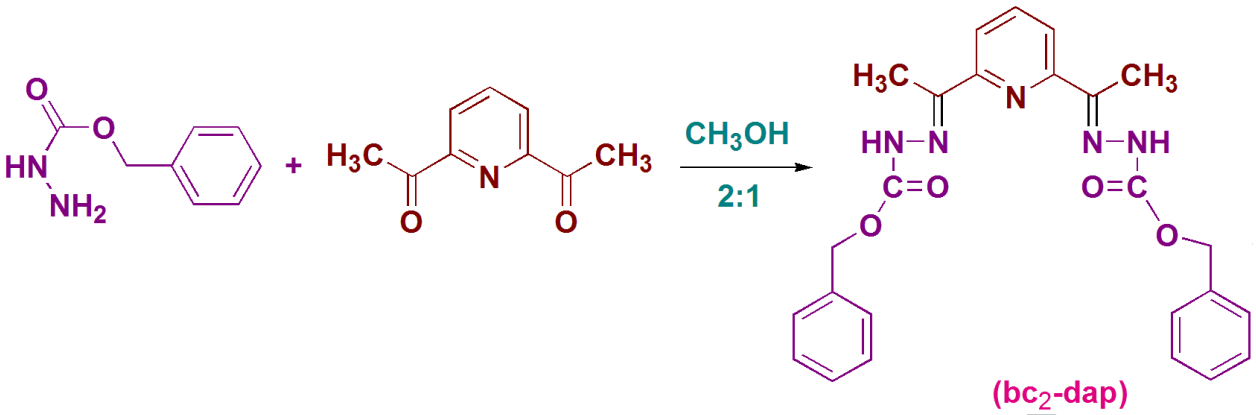


**Scheme 1**

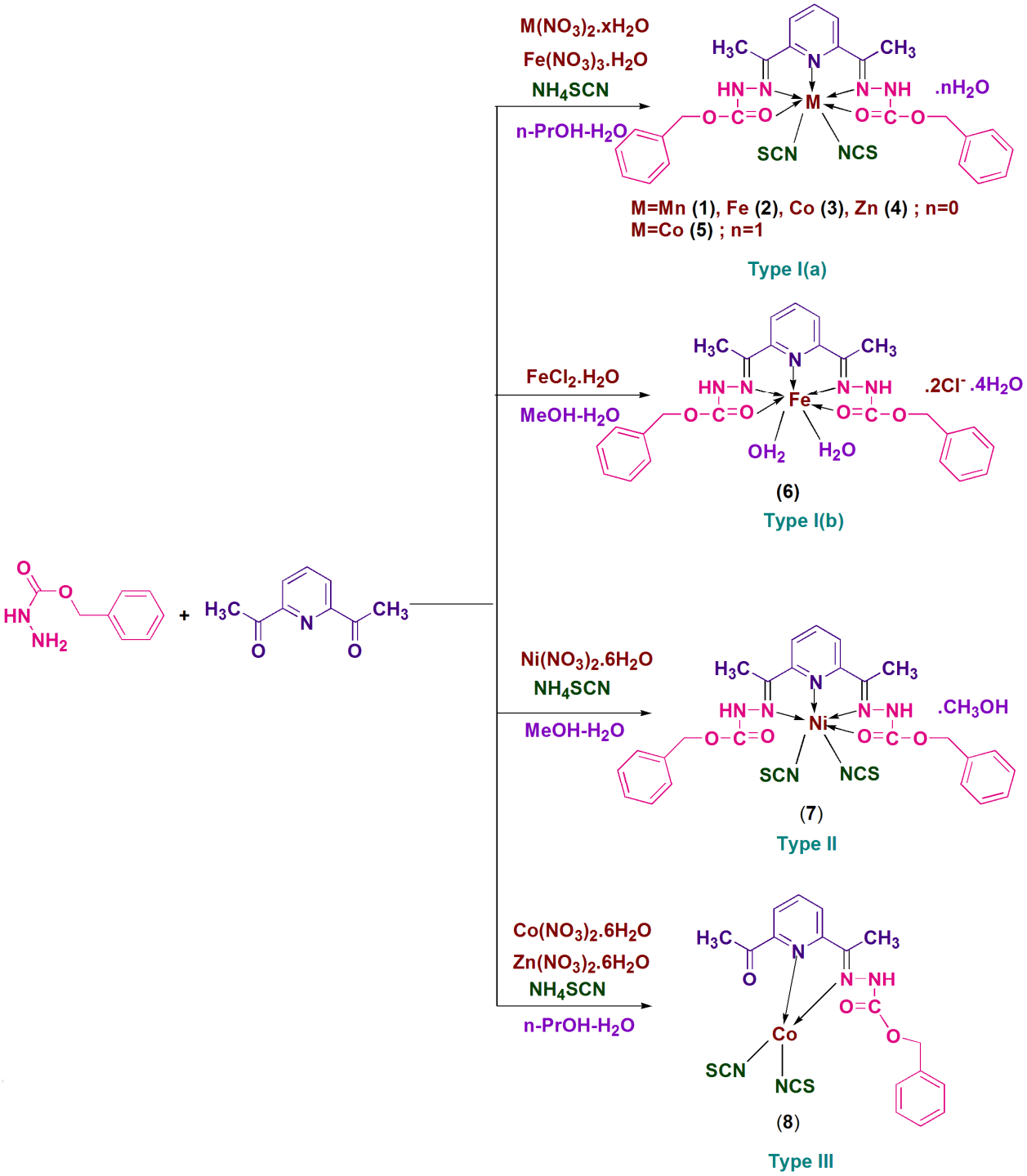


**Scheme 2**

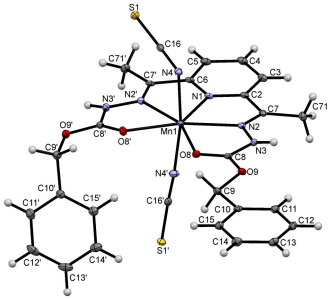

**Fig. 1a**

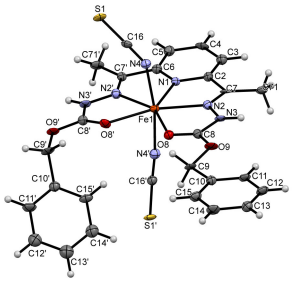

**Fig. 1b**

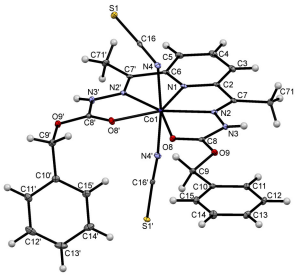

**Fig. 1c**

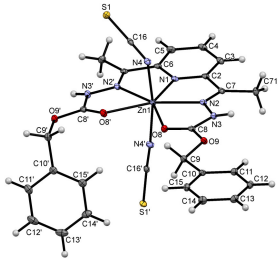

**Fig. 1d**

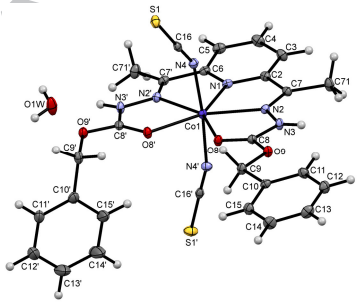

**Fig. 1e**

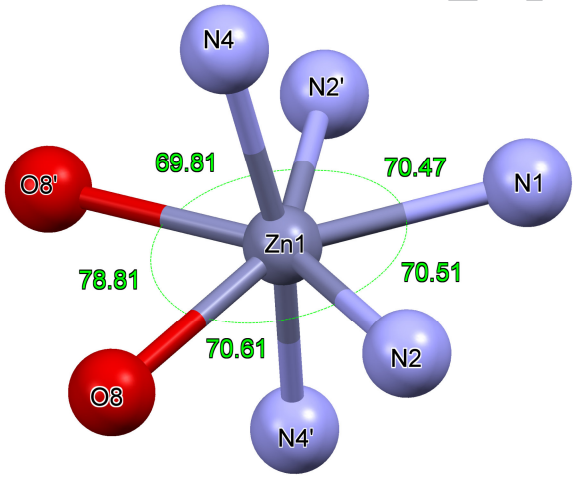


**Fig. 2**

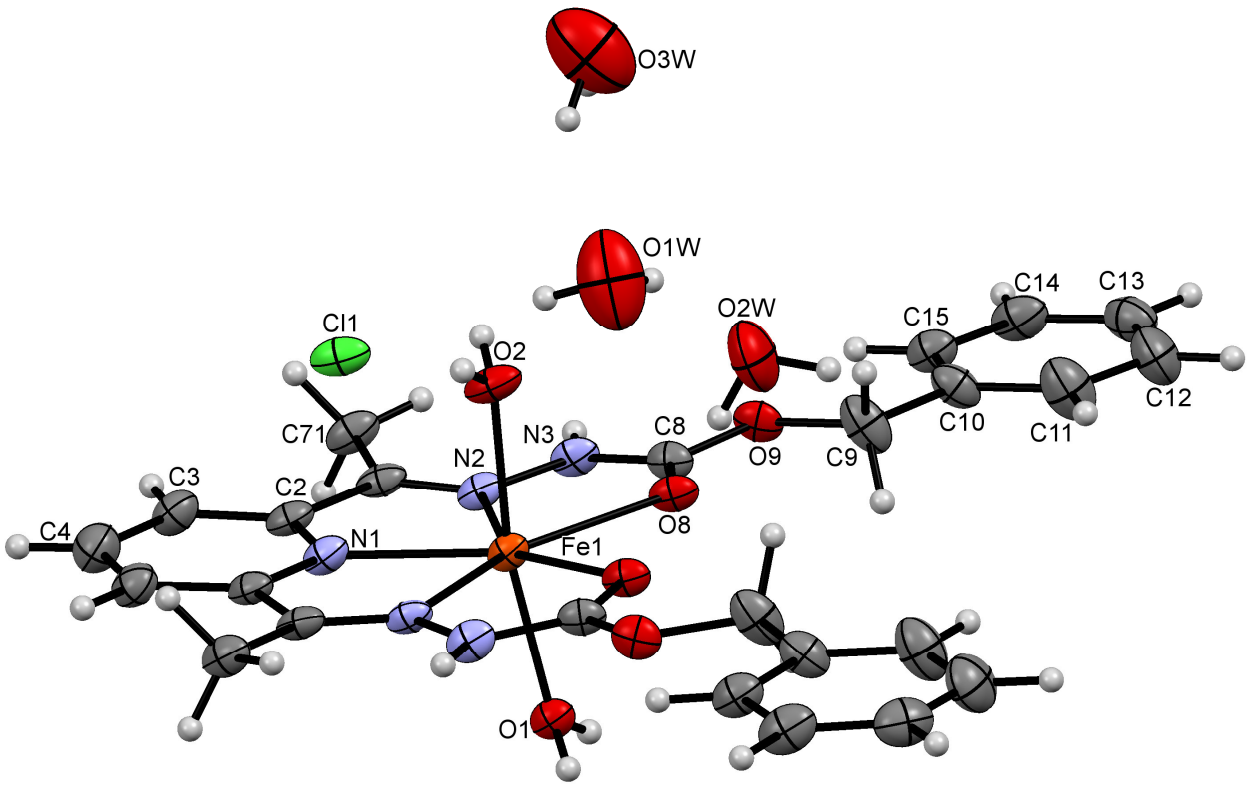
O3W
O1W
O2W
Cl1
O2
C71
N2
N3
C8
O9
C9
C15
C14
C13
C12
C10
C11
C3
C2
C4
N1
Fe1
O8
O1

**Fig. 3**

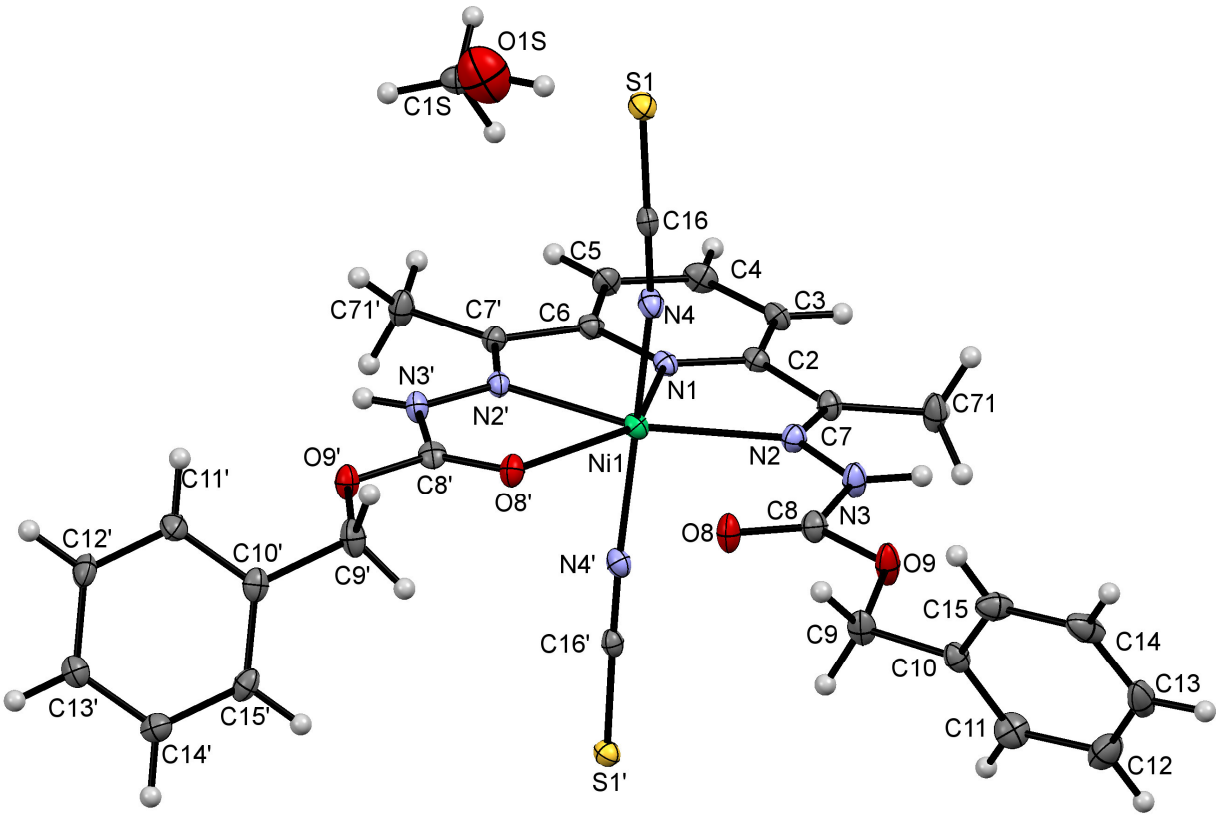


**Fig. 4**

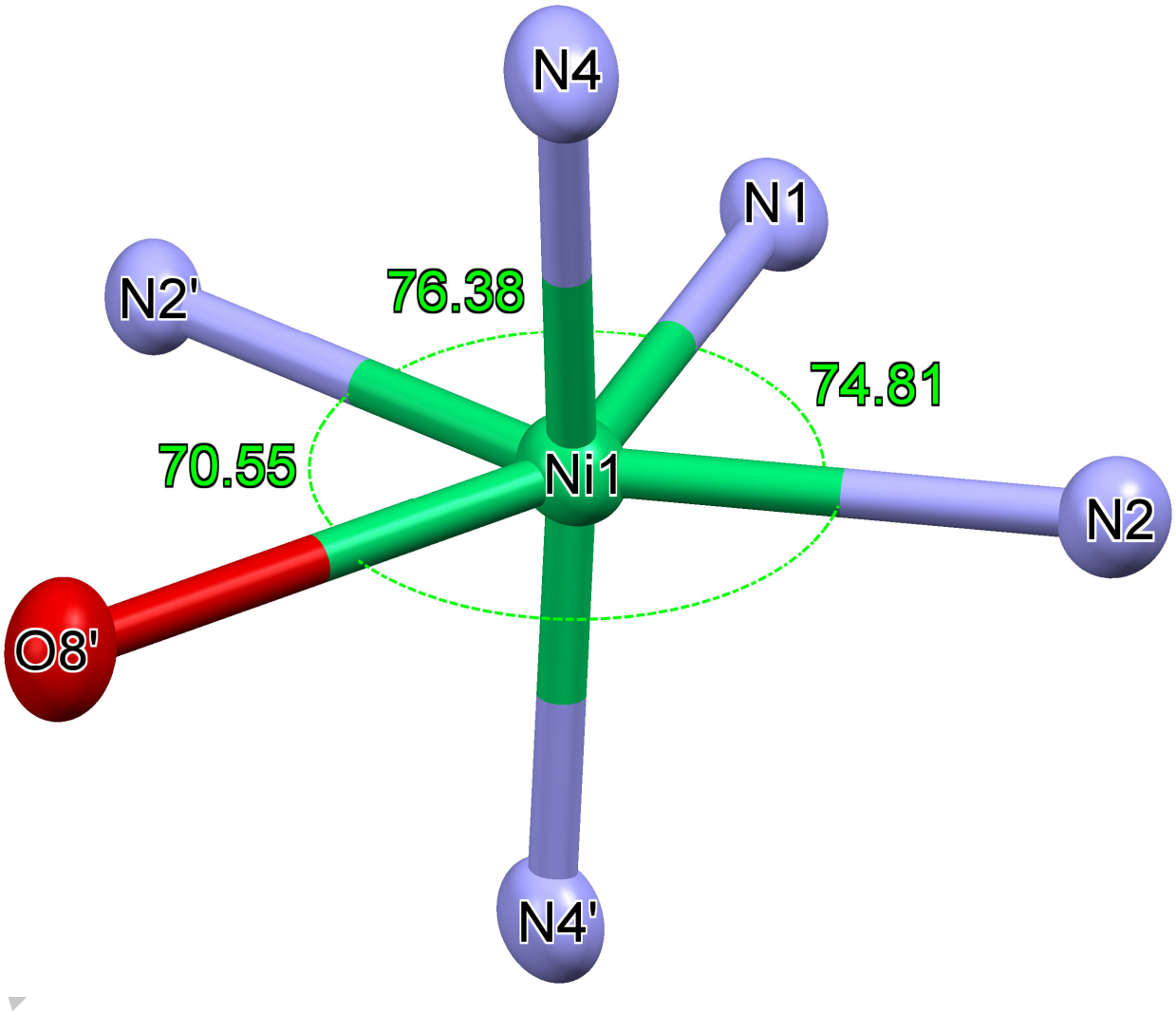


**Fig. 5**

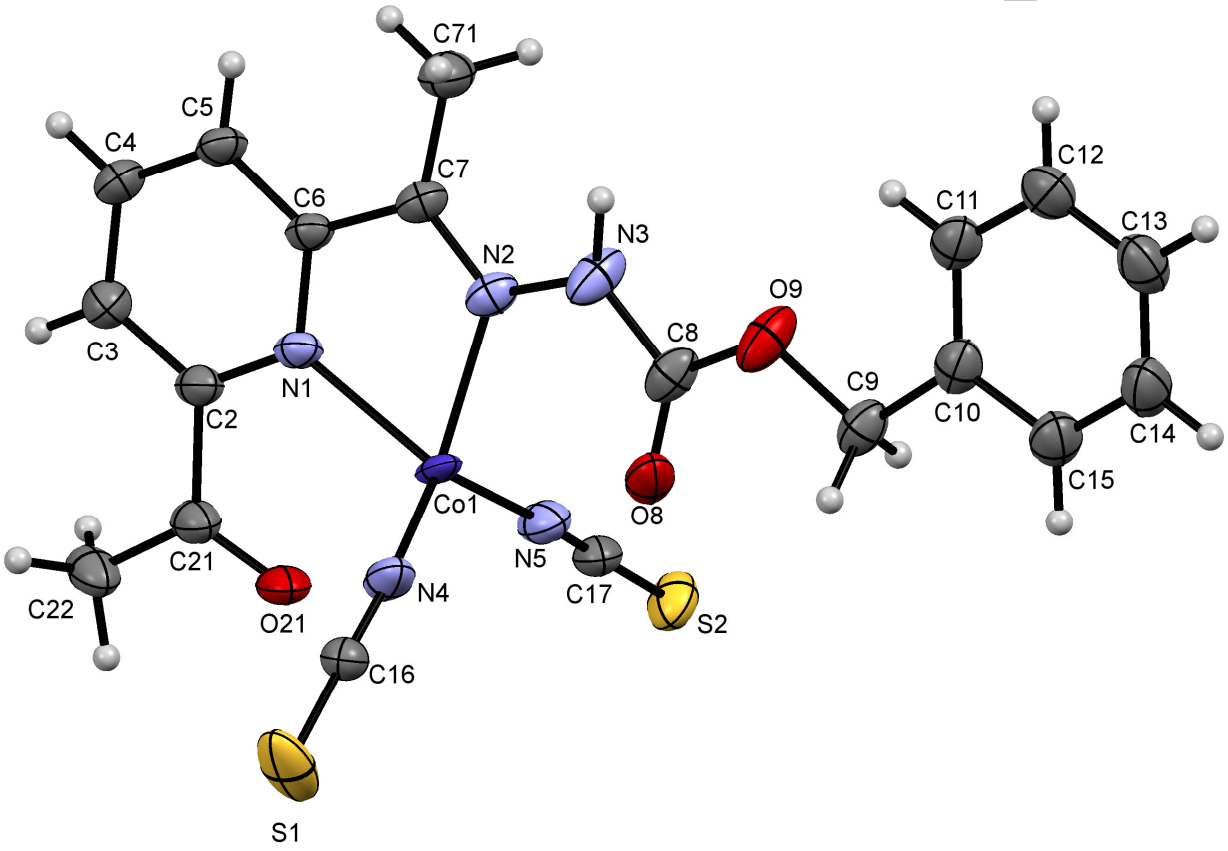


**Fig. 6**

**Table 1**: Crystal data and structure refinement parameters for complexes **1-5**

| | **1** | **2** | **3** | **4** | **5** |
|---|---|---|---|---|---|
| Empirical formula | $C_{27}H_{25}MnN_7O_4S_2$ | $C_{27}H_{25}FeN_7O_4S_2$ | $C_{27}H_{25}CoN_7O_4S_2$ | $C_{54}H_{50}Zn_2N_{14}O_8S_4$ | $C_{27}H_{27}CoN_7O_5S_2$ |
| Formula weight | 630.60 | 631.51 | 634.59 | 1282.06 | 652.60 |
| Temperature (k) | 100(2) | 100(2) | 100(2) | 100(2) | 100(2) |
| Wave length (Å) | 1.54184 | 1.54184 | 1.54184 | 1.54184 | 0.71073 |
| Crystal system | monoclinic | monoclinic | monoclinic | monoclinic | monoclinic |
| Space group | $P2_1/n$ | $P2_1/n$ | $P2_1/n$ | $P2_1/n$ | $P2_1/n$ |
| Unit cell dimensions | | | | | |
| a (Å) | 9.0530(1) | 9.1272(6) | 9.16846(12) | 9.1223(2) | 14.4546(4) |
| b (Å) | 10.3088(1) | 10.3246(5) | 10.30357(17) | 10.2603(3) | 13.8224(4) |
| c (Å) | 29.8502(4) | 29.4188(15) | 29.2319(4) | 29.5432(8) | 14.9715(3) |
| α (˚) | 90 | 90 | 90 | 90 | 90 |
| β (˚) | 90.314(1) | 91.014(5) | 91.4182(12) | 90.951(3) | 93.811(2) |
| γ (˚) | 90 | 90 | 90 | 90 | 90 |
| Volume ($Å^3$) | 2785.75(6) | 2771.8(3) | 2760.63(7) | 2764.78(13) | 2984.65(13) |
| Z | 4 | 4 | 4 | 2 | 4 |
| Density (diffrn.) Mg $mm^{-3}$ | 1.504 | 1.513 | 1.527 | 1.540 | 1.452 |
| Absorption coefficient ($mm^{-1}$) | 5.659 | 6.178 | 6.696 | 3.053 | 0.764 |
| F (000) | 1300 | 1304 | 1308 | 1320 | 1348 |
| Crystal size ($mm^3$) | 0.40×0.16×0.15 | 0.33×0.27×0.24 | 0.36×0.30×0.14 | 0.47×0.22×0.12 | 0.54×0.36×0.31 |
| Reflections collected | 12545 | 19900 | 22592 | 23205 | 25040 |
| Independent reflections/$R_{int}$ | 5625/0.0381 | 5454/0.1216 | 5740/ 0.0521 | 5760/0.0314 | 6605/0.0342 |
| Completeness to theta = 67.684˚ (Cu) 25.242˚ (Mo) | 99.0 % | 100.0 % | 100.0 % | 99.9 % | 99.5 % |
| Absorption correction | multi-scan | multi-scan | multi-scan | multi-scan | multi-scan |
| Data/restraints/ parameters | 5625/0/378 | 5454/60/378 | 5740/0/378 | 5760/0/378 | 6605/0/393 |
| Goodness-of-fit on $F^2$ | 1.027 | 1.133 | 1.039 | 1.037 | 1.080 |
| R1 | 0.0440 | 0.1222 | 0.0434 | 0.0287 | 0.0367 |
| wR2 | 0.1161 | 0.3177 | 0.1134 | 0.0771 | 0.0812 |
| Largest diff. peak and hole ($eÅ^{-3}$) | 0.695 and -0.598 | 2.234 and -1.643 | 0.873 and -0.852 | 0.365 and -0.412 | 0.356 and -0.466 |

* = theta value

**Table 2**: Crystal data and structure refinement for complexes **6-8**

| | **6** | **7** | **8** |
|---|---|---|---|
| Empirical formula | $C_{25}H_{37}Cl_2FeN_5O_{10}$ | $C_{28}H_{29}N_7NiO_5S_2$ | $C_{19}H_{17}CoN_5O_3S_2$ |
| Formula weight | 694.39 | 666.41 | 486.42 |
| Temperature (K) | 100(2) | 100(2) | 100(2) |
| Wave length (Å) | 0.71073 | 1.54184 | 1.54184 |
| Crystal system | monoclinic | orthorhombic | monoclinic |
| Space group | $P2_1/m$ | $P2_12_12_1$ | $P2_1/c$ |
| Unit cell dimensions | | | |
| a (Å) | 7.2775(4) | 9.7086(2) | 9.7274(3) |
| b (Å) | 17.6983(9) | 9.8794(2) | 15.8796(3) |
| c (Å) | 12.0917(9) | 31.2512(7) | 14.1687(4) |
| α (˚) | 90 | 90 | 90 |
| β (˚) | 99.766(6) | 90 | 103.432(3) |
| γ (˚) | 90 | 90 | 90 |
| Volume ($Å^3$) | 1534.83(16) | 2997.46(12) | 2128.73(10) |
| Z | 2 | 4 | 4 |
| Density (diffrn.) Mg $mm^{-3}$ | 1.498 | 1.477 | 1.518 |
| Absorption coefficient ($mm^{-1}$) | 0.727 | 2.665 | 8.425 |
| F (000) | 724 | 1384 | 996 |
| Crystal size ($mm^3$) | 0.42×0.32×0.29 | 0.28×0.26×0.18 | 0.38×0.17×0.11 |
| Reflections collected | 9610 | 15899 | 15705 |
| Independent reflections/$R_{int}$ | 3814/0.0304 | 5462/0.0383 | 4197/0.0583 |
| Completeness to theta = 25.242 ˚ (Mo) 67.684 ˚ (Cu) | 99.6 % | 99.9 % | 99.9 % |
| Absorption correction | multi-scan | multi-scan | multi-scan |
| Data/restraints/ parameters | 3814/6/228 | 5462/0/399 | 4197/0/276 |
| Goodness-of-fit on $F^2$ | 1.178 | 1.048 | 1.090 |
| R1 | 0.0739 | 0.0411 | 0.0702 |
| wR2 | 0.1542 | 0.1009 | 0.1941 |
| Largest diff. peak and hole ($eÅ^{-3}$) | 1.452 and -0.811 | 0.316 and -0.544 | 1.695 and -0.815 |

**Graphical Abstract:**

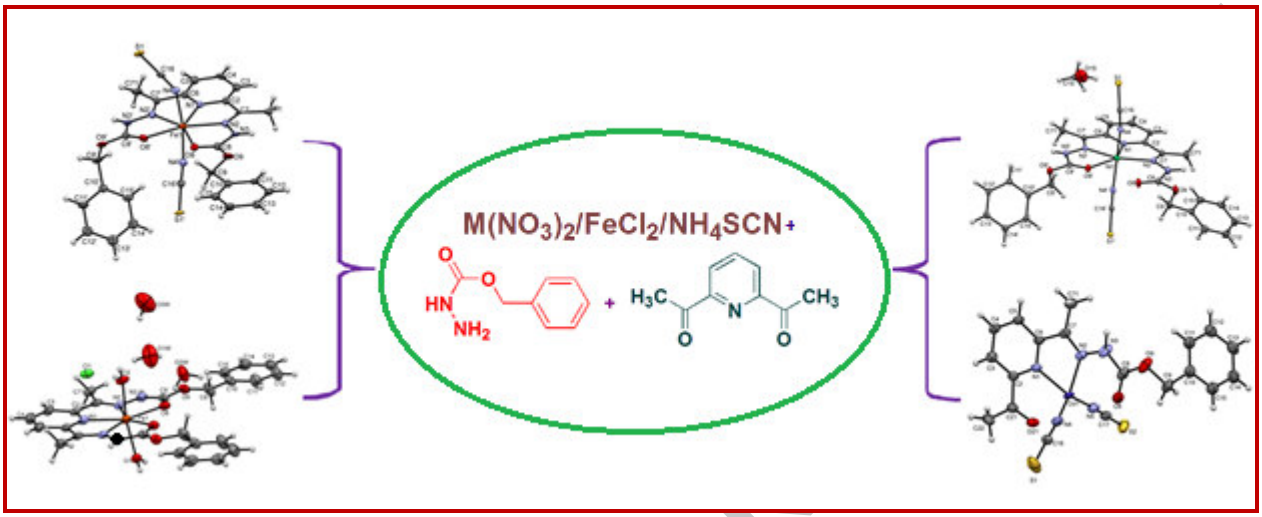


**Synopsis:**

Schiff base ligand derived from benzyl carbazate and 2,6-diacetylpyridine and its complexes have been synthesized. All the complexes were characterized by single crystal X-ray diffraction studies. The thermal properties of the complexes have been investigated by TG-DTA which designates that metal oxide is formed as the final residue.